Numerical Analysis onto Thermal Balance Behaviors of Motorized Spindle Unit

Yifan Zhang
Teng Liu (wuqiu-liu@163.com)
Tianjin University
Weiguo Gao
Jianjun Zhang
Dawei Zhang

Research Article

Keywords: Motorized spindle unit, Power matching, Thermal balance, Heat-fluid-solid coupling, GA-ELM

Posted Date: May 23rd, 2022

DOI: https://doi.org/10.21203/rs.3.rs-1650750/v1

Numerical Analysis onto Thermal Balance Behaviors of Motorized Spindle Unit

Yifan Zhang[1], Teng Liu[2, 3*], Weiguo Gao[3], Jianjun Zhang[2], and Dawei Zhang[3]

[1] *School of Computer Science and Technology, Civil Aviation University of China, Tianjin 300300, China*

[2] *School of Mechanical Engineering, Hebei University of Technology, Tianjin 300130, China*

[3] *Key Laboratory of Mechanism Theory and Equipment Design of Ministry of Education, Tianjin University, Tianjin 300355, China*

Abstract: Generally, the accuracy stability of precision motorized spindle unit is influenced by its structural thermal balance behaviors (power matching degree of spindle structural heat generations - dissipations). For the accurate analysis onto this spindle heat transfer behaviors based on temperature detections, this paper describes a method constructed with the numerical simulation technology and a proposed GA-ELM algorithm. Firstly, heat-fluid-solid coupling FE transient model is established to simulate spindle thermal behaviors, its thermal loads / boundary conditions are initially according to empirical calculations. Secondly, based on spindle temperature detections, these initial values are applied onto thermal simulations and corrected by GA, to make simulated spindle temperatures gradually approach detections. Specially, ELM is adopted to estimate the functional relationships from parent population to child population generated by genetic operators with the increasing fitness values, and the trained ELM model is utilized to ensure the GA faster convergence. Eventually, based on the corrected thermal load / boundary condition values and simulation results, the time-varying power matching conditions of spindle structural heat generation - dissipation are analyzed. This study provides a theoretical basis for the optimization and promotion of spindle structural design and coolant control strategy.

Keywords: Motorized spindle unit, Power matching, Thermal balance, Heat-fluid-solid coupling, GA-ELM

*E-mail address of the corresponding author: wuqiu-liu@163.com

1 Introduction

As the core component of precision machining tools, the motorized spindle unit always has a serious thermal impact onto the machine accuracy and accuracy stability [1-2]. When a motorized spindle unit is in machining activities, its thermal deformation errors are always caused by the heat generations of its built-in motor and bearings, owing to the compact spindle structure. Meanwhile, for the machining workshop, the ambient air convection with time-varying temperature contributes the spindle structural thermal imbalance and thermal errors as well. For these problems, recirculation coolants are always adopted into the spindle structural design for improving its thermal behaviors, and potentially realize the accurate dissipations onto these heat transfers to correct spindle thermal errors [3-4]. Based on this background, a quantitative investigation onto the power matching degrees of spindle heat generations - dissipations is theoretically vital to the optimization and promotion of spindle structural design and coolant control strategy.

On the other hand, the numerical simulation modeling technology allows engineers to have a deep and direct knowledge about spindle structural thermal behaviors [5]. Thus, the accurate modeling based on spindle thermal simulation is critical for this thermal observation. However, empirical calculations of spindle heat loads (heat generations) and boundary conditions (heat convection coefficients) are always distinct with their real values. This is the main factor causing the inaccuracy of spindle thermal simulation [6]. Therefore, to construct an optimal algorithm method for the accurate correction of thermal simulation loads / boundary conditions, to make the simulated spindle temperatures close to the temperature detections, is the necessary preparation for numerical analyses onto spindle thermal balance behaviors of spindle structure.

Over latest years, scholars adopted numerical simulation technology to analyze thermal behaviors of various motorized spindle units. Liu et al. [7] presented the thermal resistance network of spindle-bearing conjunction for spindle thermal simulation modeling, to simulate its thermal behaviors. Zivkovic et al. [8] established the spindle thermal simulation model based on the thermo-structure coupling method, and then systematically study the influences from bearing stiffness characteristics onto spindle temperature and thermal errors. Lee et al. [9] investigated the association between spindle vibration behaviors and thermal errors by an established numerical model of spindle thermal behaviors. Gao et al. [10] presented a simulation modeling method to investigate the multi-physics coupling phenomenon of aerostatic spindle system. Shi et al. [11] utilized the Volume of Fluid method combined with the Lee phase change model to realize the numerical simulation of a loop rotating heat pipe with

the two-bend structure, which aims to cool the shaft of high-speed motorized spindle. Liu et al. [12] established a CNC lathe spindle-bearing model considering the thermal effect to predict the dynamic characteristics of spindle system. The dynamic differential equation of this model is built by finite element method. Although these models above reflect thermal behaviors of motorized spindle unit in some degrees, the correction or optimization of thermal loads and boundary conditions are scarcely considered in them.

Some other scholars adopted the detections based thermal simulation methods to calculate or correct loads / boundary conditions for accurate thermal balance analysis onto various spindle structures. Huang et al. [13] determined the time-dependent heat flux generated in rotor and stator for the high-speed electric motor by an inverse algorithm utilizing the steepest descent method onto the spindle thermal simulation model. Li et al. [14] presented a method based on radial basis function neural network to calculate thermal boundary conditions for simulation onto temperature fields / thermal deformations of a motorized spindle system. Huang et al. [15] presented an efficient inverse method for estimating time-varying heat generations of spindle bearings under various working conditions, by the ANSYS parametric design language and the conjugate gradient method. Tan et al. [16] proposed a surrogate assisted differential evolution method to obtain accurate convective heat transfer coefficients in finite element thermal analysis of motorized spindle unit. Although these studies have contributed to accurate numerical simulation for spindle thermal behaviors, they are lacking in accurate analyses onto the real-time power matching relationship of spindle structural heat generations - dissipations.

This paper describes a temperature detection based correcting method onto the transient loads / boundary conditions for thermal simulations of motorized spindle unit for its thermal balance analysis, based on the numerical simulation technology and a proposed GA-ELM algorithm. The organization of this paper is as follows: Being the preparations, Section 2 establishes the heat-fluid-solid coupling simulation model for the spindle thermal behaviors, and Section 3 describes the spindle temperature detection method. On the simulation and experiment bases, Section 4 presents the optimal correction procedure onto transient loads / boundary conditions for accurate thermal simulations of motorized spindle unit, based on GA and ELM algorithms. After the corrections, Section 5 verifies the accuracy of the corrected thermal simulation modeling of spindle structure, and then gives the method onto power matching analyses of spindle heat generations - dissipations in operations. Section 6 concludes the whole study.

2 Heat-fluid-solid coupling simulation modeling of motorized spindle unit

2.1 Calculations of heat loads / boundary conditions for spindle thermal simulation

2.1.1 Heat generation calculations of motorized spindle unit

It can be seen in Fig. 1 that, heat generating parts of motorized spindle unit mainly include the front / rear bearing groups and motor. The motor consists of stator and rotor, and its heat generation is mainly due to the mechanical and electromagnetic loss. The bearing heat generation is mainly owing to the friction of the rollers-inside / outer rings and bearing-lubricating fluids. Empirical calculation methods of heat generations of spindle motor and bearings are as follows.

(1) Heat generation calculation of spindle motor

Heat generations of rotor and stator account for about 1/3 and 2/3 of the motor total heat generation respectively. They can be calculated as follows:

First of all, the effective input power of spindle motor Q_{in} (W) is:

$$Q_{\text{in}} = \sqrt{3}UI\cos\alpha \tag{1}$$

Where, U is the spindle rated voltage (V), I is the spindle rated current (A), cosα represents the motor power factor.

Besides, the power loss of spindle motor ΔQ (W) is:

$$\Delta Q = Q_{\text{in}}\left(1-\eta\right) \tag{2}$$

Where, η is the efficiency of spindle motor.

Lastly, the power loss (heat generation) of the rotor / stator in spindle motor is:

$$\begin{cases} Q_{\text{ro}} = \dfrac{1}{3}\Delta Q \\ Q_{\text{st}} = \dfrac{2}{3}\Delta Q \end{cases} \tag{3}$$

Where, Q_{ro} and Q_{st} represents heat generation powers of motor rotor and stator respectively (W).

(2) Heat generation calculation of spindle bearings

For the spindle operation, the spindle bearing roller rolls at high speed in the inner / outer ring raceway due to the speed difference between bearing internal and external rings. This high-speed rotation results in that, bearings generate heat due to rolling friction above and viscous friction between bearings-lubricating fluids.

The heat produced by the rolling friction between the bearing roller and the inner / outer ring raceway Q_{be} (W) is:

$$Q_{be} = 1.047 \times 10^{-4} Mn \tag{4}$$

Where, Q_{be} is the heat generated by bearing friction (W), M is the friction torque between bearing and raceway / lubricant (N·mm), and n represents bearing speed (RPM).

Bearing friction torque M is related to friction torque M_0 (N·mm) and friction torque M_1 (N·mm). Specially, M_0 is related to lubricating fluid viscosity and M_1 to force load. They can be calculated as follows:

$$M = M_0 + M_1 \tag{5}$$

The friction torque M_0 is:

$$\begin{cases} M_0 = 160 \times 10^{-7} f_0 d_m, & \left(v_0 n < 2000\right) \\ M_0 = 1 \times 10^{-7} f_0 \left(v_0 n\right)^{\frac{2}{3}} d_m, & \left(v_0 n \geq 2000\right) \end{cases} \tag{6}$$

Where, f_0 is the empirical coefficient related to bearing lubrication mode and bearing type, v_0 is the motion viscosity of lubricating fluid under the current working conditions (mm^2/s), and d_m is the diameter of bearing pitch circle (mm).

The friction torque M_1 is:

$$M_1 = f_1 F_\beta d_m \tag{7}$$

Where, f_1 is the empirical coefficient related to bearing force load and bearing type, and F_β is calculation load for determining the friction torque of bearings (N).

2.1.2 Heat dissipation calculations of motorized spindle unit

The heat dissipation onto motorized spindle unit includes both the forced and natural convection heat transfers, which is revealed in Fig. 2: The part where the natural convection occurs with ambient air is mainly the spindle shell. Meanwhile, because of the high-speed rotation, the spindle shaft and inspection rod force their surrounding air to flow rapidly. Thus, the air forced convective heat transfer occurs around them (including the motor stator - rotor clearance). In addition, helical channels are filled with flowing coolants, so the forced convective heat transfer also occurs in them.

The forced convective heat transfer coefficient of solid surfaces with air h (W/(m^2·K)) can be calculated as follows:

$$h = \frac{Nu_a \lambda_a}{d_e} \tag{8}$$

Where, Nu_a is the Nusselt number of air, λ_a is the thermal conductivity of air (W/(m·K)) and d_e is the equivalent diameter of rotating surface (mm).

The Nusselt number Nu_a is:

$$Nu_a = 0.133 Re_a^{\frac{2}{3}} Pr_a^{\frac{1}{3}} \tag{9}$$

Where, Re_a is Reynolds number and Pr_a is Prandtl number.

The Reynolds number Re_a is:

$$Re_a = \frac{V_a d_e}{v_a} \tag{10}$$

Where, V_a is the linear velocity of rotating body surface relative to the surrounding air (m/s), v_a is the kinematic viscosity of air (m^2/s).

The Prandtl number Pr_a is:

$$Pr_{\mathrm{a}} = \frac{C_{\mathrm{a}}\mu_{\mathrm{a}}}{\lambda_{\mathrm{a}}} \tag{11}$$

Where, C_{a} is the specific heat capacity of air (J/(kg·K)), μ_{a} is the dynamic viscosity of air (N·s/m^2).

On the solid surface where natural convection occurs with ambient air (spindle shell), the natural convective heat transfer coefficient is 9.7 W/(m^2·K) [17].

2.2 Finite element simulation modeling of thermal behaviors of motorized spindle unit

2.2.1 Spindle CAD model and its meshing

As illustrated in Fig.3, the simplified CAD model of motorized spindle unit is established and meshed in Fluent. For meshing, the spindle structure generates a total of 97013 grid nodes and 456187 grid units, of which the fluid part (Coolants #1-6 in Fig. 3(b)) of motorized spindle unit contains 4456 grid nodes and 7944 grid units.

2.2.2 Solution of heat-fluid-solid coupling simulation of motorized spindle unit

After the meshing onto spindle CAD model above, concerned fluid and solid material properties in Tab. 1 are assigned into their respective regions. Besides, heat-fluid-solid coupling FE simulation for the spindle thermal balance behaviors must be based on considerations of 2 critical contact thermal resistances: bearing outer ring - housing joint (6.06e-4 m^{2}K/W) and bearing inner ring - shaft joint (1.37e-4 m^{2}K/W). Determinations of thermal resistance values for critical spindle joints were by experimental methods [18].

In order to ensure the coolant continuity for spindle front and rear bearing groups, Coolants #1-3 and #4-5 (Fig. 3(b)) are set to be connected head to tail in sequence respectively, which is realized by UDF. Besides, for simulating the interaction effects between spindle heat generations and coolant heat dissipations by the finite element technology, the mathematical model of heat-fluid-solid coupling must be considered. The heat generation process and fluid-solid conjugate heat transfer are obtained by solving the equation (12) [19]:

$$\frac{\partial}{\partial t}\left(\rho_{\mathrm{oil\_sol}} H_{\mathrm{en}}\right) + \nabla \bullet \left[\vec{v}\left(\rho_{\mathrm{oil\_sol}} H_{\mathrm{en}} + p\right)\right] = \nabla \bullet \left[k_{\mathrm{oil\_sol}} \nabla T + \left(\bar{\bar{\tau}}\,\vec{v}\right)\right] + S_{\mathrm{h}} \tag{12}$$

Where, ρ_{oil_sol} is the density of coolant oil or solid structure (kg/m^3), k_{oil_sol} is the thermal conductivity of coolant oil or solid structure (W/(m·K)), H_{en} is the energy content per unit mass (J), p is the pressure (Pa), $\vec{v}$ / $\overline{\overline{\tau}}$ is the velocity vector/ stress tensor, S_h is the heat generation power of volumetric heat source (W), $\nabla \bullet \left(\overline{\overline{\tau}} \vec{v}\right)$ is the viscous power dissipation of flowing coolant (W), $\nabla \bullet \left(k \nabla T\right)$ is the heat transfer among solid, flowing coolant and ambient air (W).

Meanwhile, the flow field is obtained by the finite element method. Since the coolant is in a laminar flow state and assumed to be a steady-state viscous incompressible fluid, the flow field is calculated by solving equation (13):

$$\begin{cases} \dfrac{\partial u}{\partial x} + \dfrac{\partial v}{\partial y} + \dfrac{\partial w}{\partial z} = 0 \\ \dfrac{\partial}{\partial t}\left(\rho_{oil} \vec{v}\right) + \nabla\left(\rho_{oil} \vec{v}\vec{v}\right) = -\nabla p + \nabla\left(\overline{\overline{\tau}}\right) \end{cases} \tag{13}$$

Where, $u/v/w$ is the coolant flowing velocity on X/Y/Z direction (m/s), and ρ_{oil} is the density of coolant (kg/m^3).

Based on this mathematical model, transient thermal simulation of motorized spindle unit can be solved in Fluent software. For this solution, the heat loads / boundary conditions (Heat generating powers of motor / bearings and forced / natural convection heat transfer coefficients) can be calculated by the empirical methods given in Section 2.1. However, these empirically calculated values are always distinct with their actual values, which leads to the simulation inaccuracy of spindle thermal behaviors.

This paper presents an accurate correction method onto these calculated heat loads / boundary conditions based on the numerical simulation and optimal algorithm, to make the simulation results more consistent with the actual detections. Thus, the spindle temperature detection is a necessary preparation for this correction.

3 Temperature detections for thermal balance analyses onto motorized spindle unit

For the actual machining activities, although spindle heat generations can be dissipated by coolants with some strategies, some rest heat being accumulated in spindle structure can cause temperature rises nearby front / rear bearing groups and motor. As revealed in Fig. 4, RTD sensors #1-4 are located onto

spindle structural shell surface nearby the parts above, and RTD sensors #5-6 are fixed to touch the outer rings of front / rear bearing groups. With the temperature detections, the motorized spindle unit is experimentally operating at the constant 3000RPM lasting for 5 hours and the progressive 1000-3000RPM (increasing step is 500RPM for each hour) respectively. Coolant supply temperatures / flow rates are set to be 22℃ / 5L/min respectively, and the ambient temperature varies within the range 18℃-22℃.

For experiments, the detected temperature rises are substantially to reveal spindle structural pure heat absorption caused by comprehensive effects of spindle heat generations, coolant dissipations and ambient air convections. These temperature detections are preparations for thermal balance analyzing method onto motorized spindle unit.

4 GA-ELM based correction algorithm onto heat loads / boundary conditions for accurate spindle thermal simulation

4.1 Optimization model for corrections onto heat loads / boundary conditions for accurate spindle thermal simulation

Heat loads / boundary conditions empirically calculated in Section 2.1 are generally distinct with their real values. For a simulation model truly reflecting the structural thermal change of motorized spindle unit under actual working conditions, these empirical values must be accurately corrected by the optimization method: To begin with, heat loads / boundary conditions obtained empirically are designed to be accurately corrected by the following method:

$$\begin{cases} Q_{\text{be/ro/st}}{}' = k_{Q\_\text{be/ro/st}} \bullet Q_{\text{be/ro/st}} + b_{Q\_\text{be/ro/st}} \\ h_{\text{ins/st-ro}}{}' = k_{\text{h\_ins/st-ro}} \bullet h_{\text{ins/st-ro}} + b_{\text{h\_ins/st-ro}} \end{cases} \tag{14}$$

Where, $Q_{\text{be/ro/st}}$ denotes heat generation powers of spindle bearing and motor rotator / stator respectively; $h_{\text{ins/st-ro}}$ stands for air heat convection coefficient of inspection rod and motor stator - rotator clearance respectively. The proportionality coefficient *k* and deviation correction coefficient *b* are utilized to accurately correct them respectively, and then must be determined based on the optimization method. The vector of design variables for optimization is:

$$\boldsymbol{X} = \left[X_1, X_2, X_3, X_4, X_5, X_6, X_7, X_8, X_9, X_{10}\right]^{\mathrm{T}} = \left[k_{Q\_\text{be}}, b_{Q\_\text{be}}, k_{Q\_\text{ro}}, b_{Q\_\text{ro}}, k_{Q\_\text{st}}, b_{Q\_\text{st}}, k_{h\_\text{ins}}, b_{h\_\text{ins}}, k_{h\_\text{st-ro}}, b_{h\_\text{st-ro}}\right]^{\mathrm{T}} \tag{15}$$

In equation (15) above, proportionality coefficients k=1 and deviation correction coefficient b=0 are used as initial values of design variables. The constraint condition is the heat transfer, fluid mechanics, structural mechanics and other multi-physical field models involved in the heat-fluid-solid coupling transient simulation of motorized spindle unit.

In the iterative optimization process, it is necessary to derive the temperature data (corresponding to monitoring locations of RTD sensors #1-6 shown in Fig. 4) at each time step of spindle heat-fluid-solid coupling simulation results. The simulation temperature data currently extracted is compared with the corresponding experimental temperature data with the same operating conditions. The optimization objective function is to satisfy the minimization of overall error e constructed with the simulation temperature T_{si} and test temperature T_{ei} in experiments at each monitoring location:

$$e = \sum_{i=1}^{6} (T_{si} - T_{ei})^2, \quad i = 1,2,...,6 \tag{16}$$

When the overall error minimization is not met, values of heat loads / boundary conditions are adjusted, and the iteration process is repeated; When the overall error meets the requirement, the iterative optimization process is completed, and then corrected heat loads / boundary conditions and accurate simulated spindle structural temperatures are output. In this paper, the iterative optimization process above is realized by a combination technology based on genetic algorithm (GA) [20] and extreme learning machine (ELM) [21].

4.2 GA -ELM based optimization algorithm onto spindle thermal simulation

4.2.1 Realization of GA algorithm based on spindle thermal simulation

Being an effective random search method for global optimum, genetic algorithm (GA) uses a population of strings to encode the initial candidate solutions. And then it employs genetic operators, including selection, mutation and crossover, to generate new populations based on the initial population, and gradually evolves towards the best solution. The main advantages of GA are its strong robustness, convergence to global optimum and parallel search capability [20]. Owing to these advantages, GA can be appropriately adopted for the optimal algorithm for accurate correction onto heat loads / boundary conditions for spindle thermal simulation.

Specially, this paper adopts the regression method to estimate nonlinear relationships from parent

population to child population generated by genetic operators with the increasing fitness values. It is self-evident that the spindle heat-fluid-solid FE simulation has a time-consuming solution. Thus, the GA optimization is performed in a series of stages (Stage I, II, …) in this paper, and the trained regression model established in the previous stage is applied into the current stage, bringing a faster GA convergence of the optimization process as a whole.

For the preparation of optimization algorithm, it is necessary to assign GA parameters: number of individuals N, maximum number of generations M, precision of variables P, crossover probability Pc, mutation probability Pm, generation gap P_G, convergence prerequisite A^{sta}, and the upper and lower deviations for random generation of design variables $\Delta X_j^{up}, \Delta X_j^{low} (j = 1, 2, ..., 10)$. Based on these preparations, the procedure of this modified GA algorithm can be described in Fig. 5:

Step 1: Based on the initial values of design variables $\boldsymbol{X}^0$=[1,0,1,0,1,0,1,0,1,0], 1st population $\boldsymbol{X}^{Gen,1}$: $\boldsymbol{X}^{Gen,N}$ (Gen=1) are generated randomly according to $D_j = \left[X_j^0 - \Delta X_j^{low}, X_j^0 + \Delta X_j^{up} \right], j = 0,1,...,10$.

Step 2: Heat loads and thermal boundary condition parameters calculated empirically are corrected by the current population according to equation (14), and then applied onto heat - fluid - solid coupling finite element simulations of spindle thermal behaviors respectively. Besides, the coolant supply temperatures / flow rates and ambient temperature are considered as well.

Step 3: Based on detected spindle temperatures, the obtained simulation spindle temperatures are used into the calculation of equation (16) above. Then based on the calculation results, the fitness values of initial solutions can be calculated respectively. Crucially, to judge whether each individual in the current population is suitable for the regression training:

If $\mathrm{Fit}^{Gen,\theta} > \mathrm{Fit}^{Gen\text{-}1,\theta}$, the mapping data $\boldsymbol{X}^{Gen\text{-}1,\theta} \rightarrow \boldsymbol{X}^{Gen,\theta}$ is reserved for the regression training (θ=1,2, …, N).

Step 4: To judge whether the absolute value of overall error of simulation - test temperatures caused by the individual who has the highest fitness in current population can meet the convergence condition:

If $|e_{\theta'}| \le A^{sta}$, to output the corresponding individual $\boldsymbol{X}^{Gen,\theta'}$ for the ultimate solution, and the GA optimization is terminated; otherwise, to perform Step 5.

Step 5: If $Gen < M$, a new population is generated according to the evolution direction provided by the fitness values (Its realizations in different stages are described in detail in Section 4.2.2); *Gen*=*Gen*+1; to perform Step 2; otherwise, to perform Step 6.

Step 6: The individual who has the highest fitness in current population $\boldsymbol{X}^{Gen,\theta'}$ is selected to be initial values of design variables for next optimization stage. The GA optimization of this stage is terminated.

4.2.2 Realization of new population generation of the modified GA

For Stage I (revealed in Fig. 6(a)), GA employs genetic operators (selection, mutation and crossover) to generate a new population $\boldsymbol{X}^{Gen+1,1}:\boldsymbol{X}^{Gen+1,N}$, based on the current population $\boldsymbol{X}^{Gen,1}:\boldsymbol{X}^{Gen,N}$ and their fitness values illustrating the evolution direction. But for Stage II, III, IV... (revealed in Fig. 6(b)), 50% individuals of the new population $\boldsymbol{X}^{Gen+1,1}\square\boldsymbol{X}^{Gen+1,\frac{N}{2}}$ are generated by the method above, but the rest individuals are directly generated by the calculation of the regression model established in the previous stage. This modification onto GA optimization can improve its convergence speed.

4.2.3 ELM based training algorithm for regression modeling for the modified GA

Extreme Learning Machine (ELM) is an advanced algorithm for training single-hidden layer feedforward neural networks (SLFN). This algorithm can avoid the iteratively tuning of the traditional neural algorithms [21]. In this paper, the ELM training is adopted for the regression modeling onto the reserved mapping data $\boldsymbol{X}^{Gen\text{-}1}\left(=\left[X_1^{Gen\text{-}1},X_2^{Gen\text{-}1},...,X_{10}^{Gen\text{-}1}\right]^{\mathrm{T}}\right)\rightarrow\boldsymbol{X}^{Gen}\left(=\left[X_1^{Gen},X_2^{Gen},...,X_{10}^{Gen}\right]^{\mathrm{T}}\right)$, which is for the modified GA above, and the applied SLFN structure (illustrated in Fig. 7) can be expressed as follows:

$$f_L(\mathbf{x})=\sum_{r=1}^{L}\beta_r G(\mathbf{a}_r,b_r,\mathbf{x}) \tag{17}$$

Where, $\mathbf{a}_r$ and b_r are learning parameters of hidden nodes, β_r is the output weight, and the activation function $G(\mathbf{a}_r,b_r,\mathbf{x})$ denotes the output of r^{th} hidden node with respect to the input $\boldsymbol{x}$.

Being the basis for estimating the nonlinear functional relationships from parent population to child

population generated by genetic operators with the increasing fitness values, the SLFN structure in Fig. 7 has 10 input nodes to stand for the vector of design variables for correction optimization (equation (15)) in the previous population $\boldsymbol{X}^{Gen\text{-}1}$. Besides, the design variables above in the current population $\boldsymbol{X}^{Gen}$ are 10 SLFN output nodes respectively.

Based on the accumulation of the reserved mapping data $\boldsymbol{X}^{Gen\text{-}1,\,\theta} \to \boldsymbol{X}^{Gen,\,\theta}$ after each stage of GA optimization, the relationship of equation (17) can be determined according to the following ELM modeling procedure:

Step 1: Hidden parameters $\mathbf{a}_r$ and b_r $\left(r=1,2,...,L\right)$ of the applied SLFN are assigned randomly.

Step 2: This SLFN approximates the mapping data collection $\aleph=\{(\mathbf{x},t)\}^{M\times N}$ with 0 error ($M\times N$ is much larger than L):

$$f_L\left(\mathbf{x}_{\alpha,\tau}\right)=\sum_{r=1}^{L}\beta_r G\left(\mathbf{a}_r,b_r,\mathbf{x}_{\alpha,\tau}\right)=\mathbf{t}_{\alpha,\tau},\alpha=1,2,...,M,\tau=1,2,...,N \tag{18}$$

Then equation (18) can be written compactly as:

$$\mathbf{H}\boldsymbol{\beta}=\mathbf{T} \tag{19}$$

Where,

$$\begin{cases}\mathbf{T}=\left[t_{1,1},...,t_{M,N}\right]^{\mathrm{T}}\\ \mathbf{H}=\mathbf{H}\left(\mathbf{a}_1,...,\mathbf{a}_L,b_1,...,b_L,\mathbf{x}_{1,1},...,\mathbf{x}_{M,N}\right)=\begin{bmatrix}G\left(\mathbf{a}_1,b_1,\mathbf{x}_{1,1}\right) & \mathrm{L} & G\left(\mathbf{a}_L,b_L,\mathbf{x}_{1,1}\right)\\ \mathrm{M} & \mathrm{O} & \mathrm{M}\\ G\left(\mathbf{a}_1,b_1,\mathbf{x}_{M,N}\right) & \mathrm{L} & G\left(\mathbf{a}_L,b_L,\mathbf{x}_{M,N}\right)\end{bmatrix}_{M\times N\times L}\\ \boldsymbol{\beta}=\left[\beta_1,...,\beta_L\right]^{\mathrm{T}}\end{cases} \tag{20}$$

Step 3: The output weights can be calculated:

$$\boldsymbol{\beta}=\mathbf{P}\left(\mathbf{H}\right)^{\mathrm{T}}\mathbf{T} \tag{21}$$

Where,

$$\mathbf{P} = \left((\mathbf{H})^{\mathrm{T}} \mathbf{H} \right)^{-1} \tag{22}$$

With the obtained $\boldsymbol{\beta} = \left[\beta_1, ..., \beta_L \right]^{\mathrm{T}}$ from equation (21) above, the SLFN output function represented in equation (17) can be applied as the regression model for calculating the individuals in current population based on the previous population, with the increasing fitness values.

4.3 Optimization correction results and discussions of spindle simulation heat loads / boundary conditions

By the modified GA optimization above, accurate values of heat generation powers and convective heat transfer coefficients of motorized spindle unit are obtained. For the rotation speed case of constant 3000RPM, heat generation powers of spindle front bearing group, rear bearing group, motor stator and motor rotor are 189.21W, 34.43W, 204.96W and 102.29W respectively. And convective heat transfer coefficients of inspection rod surface and motor stator - rotator clearance are 50.1W/(m^2·K) and 123.3W/(m^2·K). Meanwhile, the values for the case of progressive 1000-3000RPM are respectively listed in Tables 2-3: Each heat generating part has the increasing heat generating power scale with the growing spindle rotation speed, and the forced convection heat transfer coefficients onto spindle structure are slightly influenced by the variations of spindle rotation speed and ambient temperature.

Based on these corrected heat generation powers and convective heat transfer coefficients, simulation temperature data of spindle structure are compared with their corresponding detected data under the constant and progressive rotation speed cases, which is shown in Fig. 8: There are agreements between spindle simulated and detected temperatures (Temperatures of front / rear bearing groups are monitored by RTD sensors #5 and #6 in Fig. 4, and temperatures of motor is detected by the spindle built-in thermal sensor). These agreements clarify that, the heat-fluid-solid coupling numerical model has the higher accuracy to simulate actual spindle thermal behaviors, based on the optimization and correction onto thermal loads and boundary conditions. This improved simulation can provide basis for the subsequent thermal balance analysis of motorized spindle units.

5 Thermal balance Analysis of motorized spindle unit

5.1 Simulation results and discussion of spindle thermal behaviors

With the working conditions described in Section 3, the simulated temperature fields of spindle structure and coolants are shown in Figs. 9-12. Blue represents the low temperature zone and red represents the high temperature zone.

It can be seen in Figs. 9-10 that, temperatures of front / rear bearings and motors are higher than that of other components of motorized spindle unit. The minimum temperature occurs at the end of spindle inspection rod, which is greatly affected by ambient temperature. The highest temperature occurs in inner ring of front bearings. This is perfectly adverse to the accuracy stability of precision motorized spindle unit. According to our previous study [22], spindle thermal deformation errors are closely related to temperature rises of spindle bearings, especially front bearings. Therefore, it is suggested that the coolant heat dissipation efficiency onto spindle front bearing group should be particularly strengthened, by some ways such as increasing coolant supply flow or reducing coolant supply temperature.

On the other hand, it can be seen that spindle structural temperatures can be obviously influenced by spindle rotation speed: As shown in Fig. 9, the structural temperature gradient of heat generating parts with constant 3000RPM rotation speed changes little with time increase (reaching approximately equilibrium). But for progressive rotation speed, spindle structural temperatures above changes greatly, which is revealed in Fig. 10.

Coolant temperature tendencies of motorized spindle unit are shown in Figs. 11-12: As described in Fig. 11, for the constant spindle speed, all coolants have the similar supply temperatures, and the motor coolant has the highest outlet temperature. The motor coolant temperature gradient is higher than front and rear bearings. These similar conditions can also be seen in the case of progressive spindle rotation speed in Fig. 12, and coolant outlet temperatures continue to rise with the speed increase. All the simulation results above are utilized to calculate the spindle heat generations and dissipations, by the method given in Section 5.2.

5.2 Power matching analysis of spindle heat generations - dissipations

5.2.1 Calculation of spindle heat generations and dissipations

After the modified GA optimization based on spindle thermal simulation introduced in Section 4, the corrected heat generation powers of spindle front / rear bearing group and motor stator / rotator (listed in Tab. 2) can be directly used into the power matching analysis of spindle heat generations - dissipations. On the other hand, heat dissipation powers of spindle structure must be calculated based

on the simulation results (Figs. 9-12) and corrected convective heat transfer coefficients (Tab. 3).

The heat dissipation onto spindle structure mainly includes the convective heat transfers from recirculation coolants and ambient air. Thus, the heat dissipation power of each spindle heat generating part can be calculated as follows:

$$\begin{cases} q_{\text{be\_fr}} = q_1 + q_2 + q_3 + q_{\text{be\_fr}}^{\text{air}} \\ q_{\text{be\_re}} = q_4 + q_5 + q_{\text{be\_re}}^{\text{air}} \\ q_{\text{mo}} = q_6 + q_{\text{mo}}^{\text{air}} \end{cases} \tag{23}$$

Where, q_{mo} / $q_{\text{be\_fr}}$ / $q_{\text{be\_re}}$ are heat dissipation powers of motor, front /rear bearing groups (W), q_1 - q_6 are the heat powers absorbed by Coolants #1-6 (shown in Fig. 3(b)) onto spindle heat generating parts (W), and $q_{\text{mo}}^{\text{air}} / q_{\text{be\_fr}}^{\text{air}} / q_{\text{be\_re}}^{\text{air}}$ are the heat powers exchanged by air convection of motor, front / rear bearings (W).

For equations (23), the heat power absorbed by coolants shown in Fig. 3(b) is:

$$q_i = c_{\text{oil}} \rho_{\text{oil}} V_{\text{s}} (T_{\text{out}} - T_{\text{in}}) \quad (i = 1, 2, ..., 6) \tag{24}$$

Where, c_{oil} is the coolant specific heat capacity (2090 J/(kg·K)), ρ_{oil} is the coolant density (910 kg/m^3), Vs is the coolant flow rate (m^3/s). T_{in} and T_{out} are the coolant inlet and outlet temperatures (°C), which must be obtained in coolant temperature simulation results (Figs. 11-12).

Besides, the heat exchanged for convective heat transfer with ambient air in equations (23) is:

$$q_j^{\text{air}} = h_{\text{f}} A_j (t_{\text{w}j} - t_{\text{f}}) \quad (j = \text{be\_fr}, \text{be\_re}, \text{mo}) \tag{25}$$

Where, h_{f} is air convection heat transfer coefficient (for natural convection: 9.7 W/(m^2·K); for forced convection: seen in Tab. 3). A is the convection heat transfer area of each heat generating part (m^2). t_{f} is ambient air temperature (°C), and t_{w} is the heat transfer surface temperature of each heat generating part (°C), which must be obtained in spindle structural temperature simulation results (Figs. 9-10).

5.2.2 Power matching degree analysis of spindle heat generations - dissipations

According to the method in Section 5.2.1, the power matching of heat generations - dissipations of motorized spindle unit can be analyzed in Fig. 13: For the constant speed case in Fig. 13 (a), the heat dissipation power of each spindle heat generating part reaches a balance in about an hour. After this state, heat generation powers of front / rear bearing group and motor are higher than their heat dissipation powers respectively. These power differences lead to temperature rises of spindle front / rear bearing group and motor, and generally cause spindle thermal deformation errors.

The similar situation can also be observed from the progressive speed case in Fig. 13 (b): With the increase of rotation speed, the heat generation power of each heat generating part of the motorized spindle unit increase gradually, and the heat dissipation power also increase correspondingly. The heat dissipation powers are always lower than heat generation powers. Each heat generating part has the poor matching degree between its heat generation and dissipation powers, which is harmful to spindle accuracy stability.

From the heat transfer perspective, the numerical method constructed by this study provides us a possibility of observing the power matching degree of heat generations - dissipations of motorized spindle unit in machining activities. That is a vital guidance onto the thermal optimization of spindle structural design and promotion of spindle coolant control strategy.

6 Conclusions

This paper establishes a heat-fluid-solid coupling simulation model of motorized spindle unit. Then based on temperature detections, a GA-ELM algorithm is proposed to correct the simulation heat load / boundary condition parameters calculated originally by empirical methods. The aim is to improve the accuracy of spindle thermal simulation, and then analyze the spindle thermal balance behaviors in machining activities. For the algorithm above, ELM is used to estimate functional relationships from parent population to child population generated by the genetic operators with the increasing fitness values, and thus to guarantee the GA faster convergence. Conclusions of this study are as follows:

1) The presented numerical analyzing method, based on the finite element simulation technology and GA-ELM algorithm, can effectively analyze the dynamic power matching state of heat generations - dissipations (heat dissipations are caused by coolant / ambient air) of motorized spindle unit. This provides the theoretical basis for the optimization and promotion of spindle structural design and coolant control strategy.

2) For the spindle structure in machining activities, the highest temperature rise generally occurs in the inner ring of its front bearing group, which is perfectly adverse to the accuracy stability of precision motorized spindle unit. It is suggested that the coolant heat dissipation efficiency onto spindle front bearing group should be particularly strengthened, by some ways such as increasing coolant supply flow or reducing coolant supply temperature.

Acknowledgment

The authors acknowledge the Fundamental Research Funds for the Central Universities (No. 3122019116).

Declarations

-Ethical Approval

Not applicable.

-Consent to Participate

All authors are consent to participate in the author team of this submitted manuscript.

-Consent to Publish

The submitted manuscript is approved by all its authors for publication.

-Authors Contributions

Yifan Zhang is the main contributor to this paper. She finished the thermal simulation modeling of motorized spindle unit. Then she designed the procedure of genetic algorithm to correct its thermal loads by optimization method, and then adopted ELM algorithm to estimate nonlinear functional relationships from parent population to child population generated by genetic operators with increasing fitness values.

Teng Liu assisted Yifan Zhang in thermal simulation of motorized spindle unit, and then improved the handwriting of the manuscript as a whole.

Weiguo Gao finished the construction of experimental platform, and then performed the contrasting experiments for this study.

Jianjun Zhang finished the data analyses about experimental and simulation results.

Dawei Zhang designed the logical structure of the whole manuscript, and then gave crucial comments onto this work for improving its technical route.

-Funding

The research was supported by the Fundamental Research Funds for the Central Universities (No. 3122019116).

-Competing Interests

No conflict of interest exits in the submission of this manuscript.

-Availability of data and materials

Data generated or analyzed in this study are available.

References

[1] Abele E, Altintas Y, Brecher C (2010) Machine tool spindle units, CIRP Annals-Manufacturing Technology. 59: 781-802.

[2] Cao HR, Zhang XW, Chen XF (2017) The concept and progress of intelligent spindles: A review, International Journal of Machine Tools and Manufacture. 112: 21-52.

[3] Chou C, DeBra DB (1990) Liquid temperature control for precision tools, CIRP Annals-Manufacturing Technology. 39: 535-543.

[4] Liu T, Gao WG, Tian YL, Zhang HJ, Chang WF, Mao K, Zhang DW (2015) A differentiated multi-loops bath recirculation system for precision machine tools, Applied Thermal Engineering. 76c: 54-63.

[5] Holkup T, Cao H, Kolar P, Altintas Y, Zeleny J (2010) Thermo-mechanical model of spindles, CIRP Annals-Manufacturing Technology. 59 (1): 365-368.

[6] Li Y, Zhao WH, Lan SH, Ni J, Wu WW, Lu BH (2015) A review on spindle thermal error compensation in machine tools, International Journal of Machine Tools and Manufacture. 95: 20-38.

[7] Liu ZF, Pan MH, Zhang AP, Zhao YS, Yang Y, Ma CY (2015) Thermal characteristic analysis of high-speed motorized spindle system based on thermal contact resistance and thermal-conduction resistance, International Journal of Advanced Manufacturing Technology. 76 (9): 1913-1926.

[8] Zivkovic A, Zeljkovic M, Tabakovic S, Milojevic Z (2015) Mathematical modeling and experimental testing of high-speed spindle behavior, International Journal of Advanced Manufacturing Technology. 77 (5): 1071-1086.

[9] Lee J, Kim DH, Lee CM (2015) A study on the thermal characteristics and experiments of high-speed spindle for machine tools, International Journal of Precision Engineering and Manufacturing. 16 (2): 293-299.

[10] Gao Q, Lu LH, Zhang R, Song LY, Huo DH, Wang GL (2019) Investigation on the thermal behavior of an aerostatic spindle system considering multi-physics coupling effect, The International Journal of Advanced Manufacturing Technology. 102 (9-12): 3813-3823.

[11] Shi XJ, Yin BT, Chen GQ, Zhang XD, Mei XS (2021) Numerical study on two-phase flow and heat transfer characteristics of loop rotating heat pipe for cooling motorized spindle, Applied

Thermal Engineering. 192 (25): 116927.

[12] Liu HY, Zhang YM, Li CY, Li ZY (2021) Nonlinear dynamic analysis of CNC lathe spindle-bearing system considering thermal effect, Nonlinear Dynamics. 105:131–166.

[13] Huang CH, Lo HC (2006) A three-dimensional inverse problem in estimating the internal heat flux of housing for high speed motors, Applied Thermal Engineering. 26: 1515-1529.

[14] Li DX, Feng PF, Zhang JF, Wu ZJ, Yu DW (2014) Calculation method of convective heat transfer coefficients for thermal simulation of a spindle system based on RBF neural network, International Journal of Advanced Manufacturing Technology. 70 (5): 1445-1454.

[15] Huang JH, Than VT, Ngo TT, Wang CC (2016) An inverse method for estimating heat sources in a high speed spindle, Applied Thermal Engineering. 105: 65-76.

[16] Tan F, Wang L, Yin M, Yin GF (2019) Obtaining more accurate convective heat transfer coefficients in thermal analysis of spindle using surrogate assisted differential evolution method, Applied Thermal Engineering. 149: 1335–1344.

[17] Xu M, Jiang SY, Cai Y (2007) An improved thermal model for machine tool bearings, International Journal of Machine Tools and Manufacture. 47 (1): 53-62.

[18] Zhao HL, Huang YM, Xu JL, Jiang LY, Zhang WH, Sheng BH (1999) Experiment research on thermal contact resistance of normal used joints, Journal of Xi'an University of Technology. 15 (3): 26-29.

[19] Anderson JD (1995) Computational fluid dynamics: the basics with applications, McGraw Hill, New York.

[20] Goldberg D E (1989) Genetic algorithm in search, optimization and machine learning, Addison-Wesley. Massachusetts.

[21] Huang GB, Zhu QY, Siew CK (2006) Extreme learning machine: theory and applications, Neurocomputing. 70 (1-3): 489-501.

[22] Liu T, Gao WG, Zhang DW, Zhang YF, Chang WF, Liang CM (2017) Analytical modeling for thermal errors of motorized spindle unit, International Journal of Machine Tools and Manufacture. 112: 53-70.

Figures

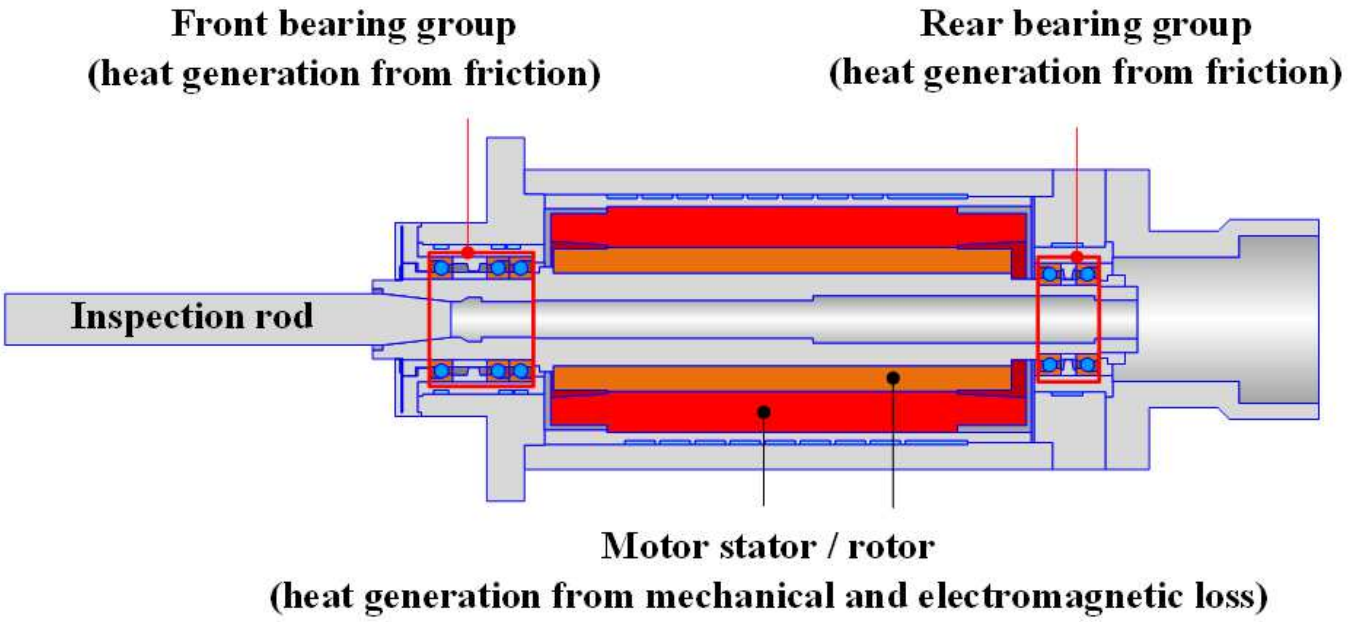

Figure 1

Heat generations of motorized spindle unit

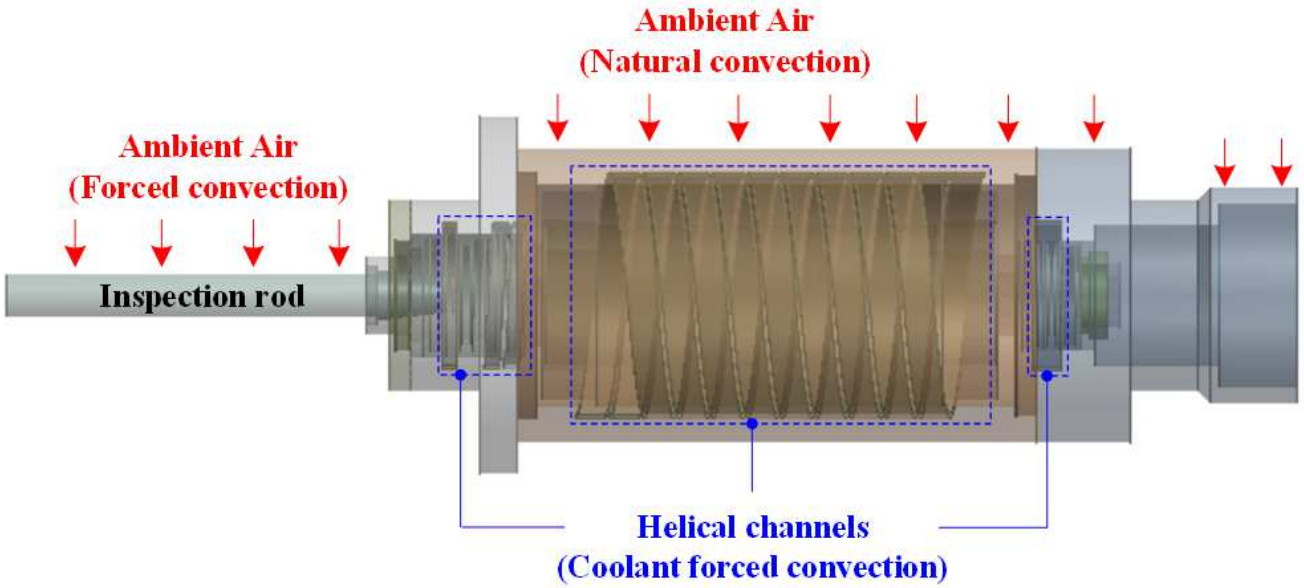

Figure 2

Heat dissipations of motorized spindle unit

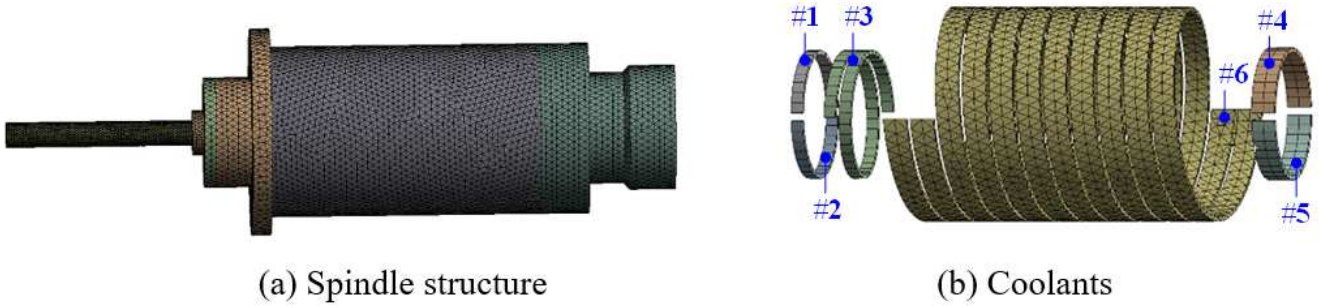

Figure 3

Meshing of spindle CAD model

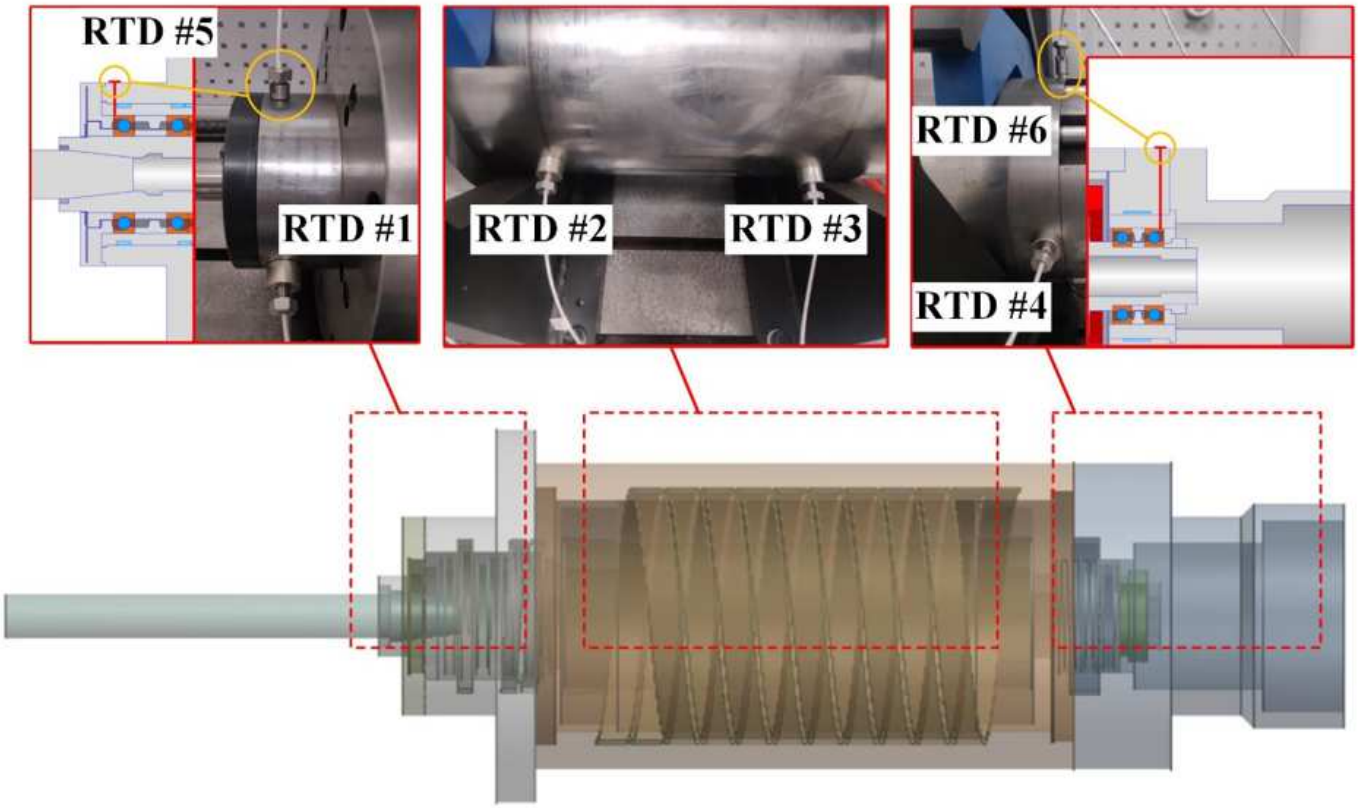

Figure 4

Spindle structural temperature detections by RTD sensors

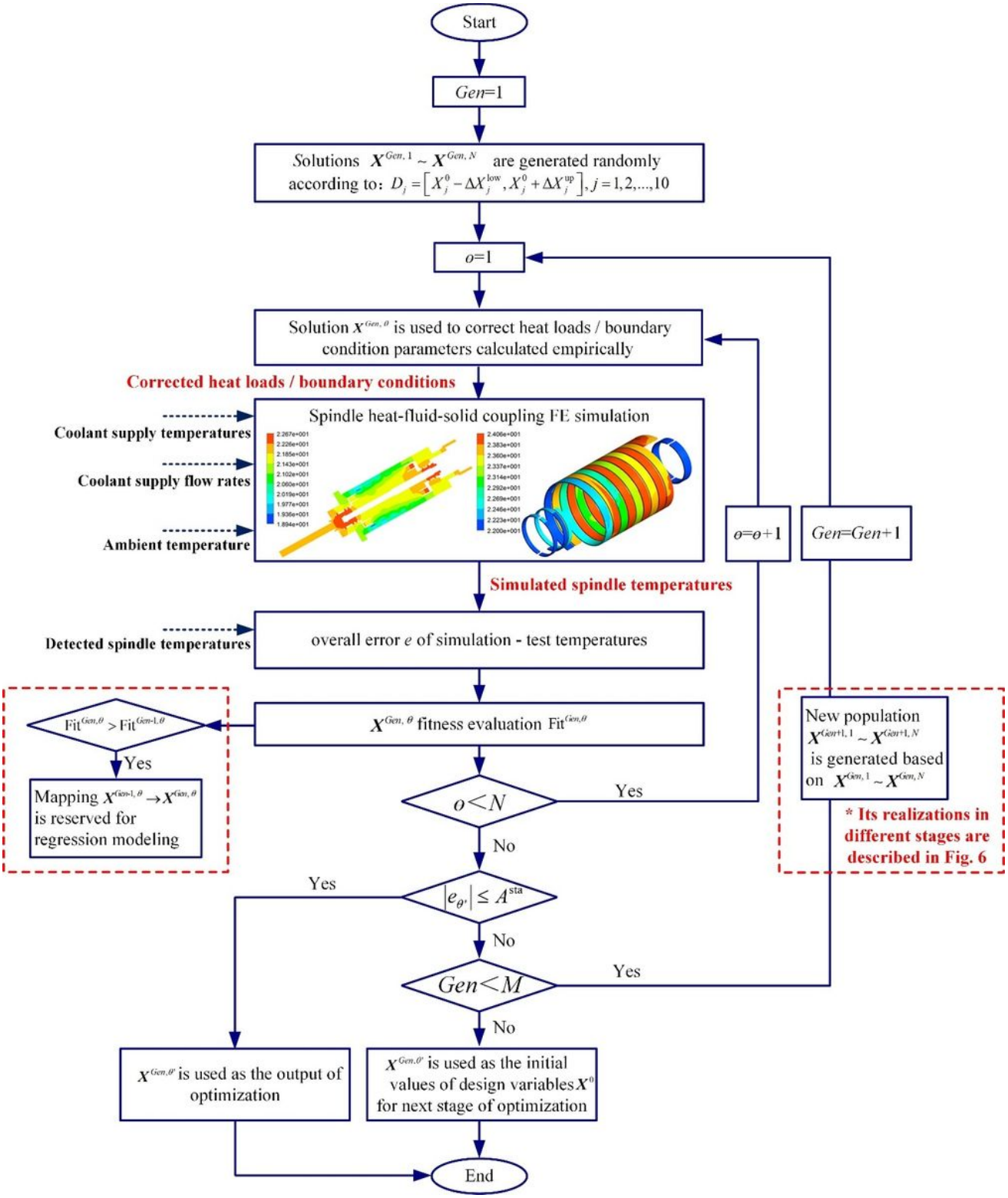

Figure 5

Modified GA optimization procedure for corrections onto heat loads / boundary conditions for spindle thermal simulations

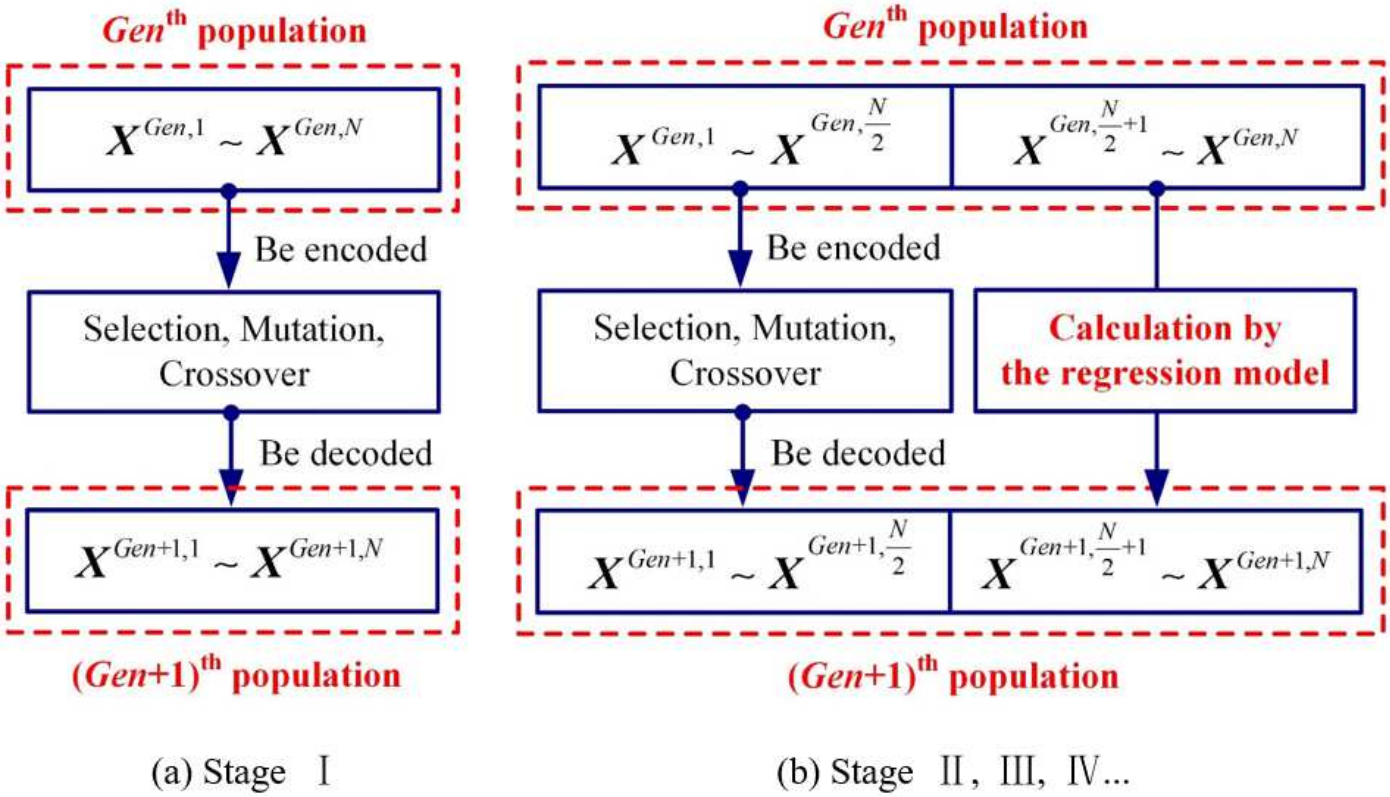

Figure 6

New population generation of the modified GA

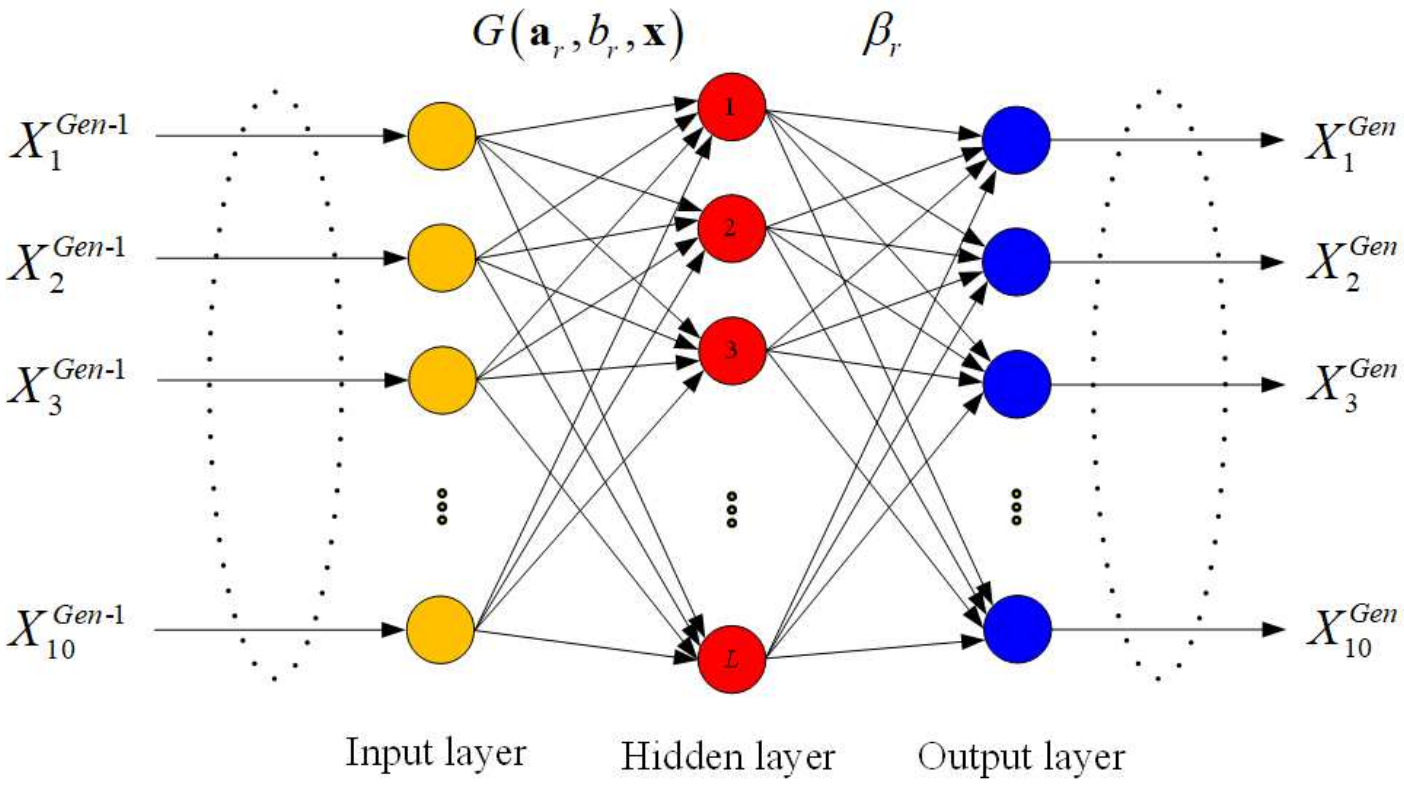

Figure 7

ELM structure applied onto regression modeling for the modified GA

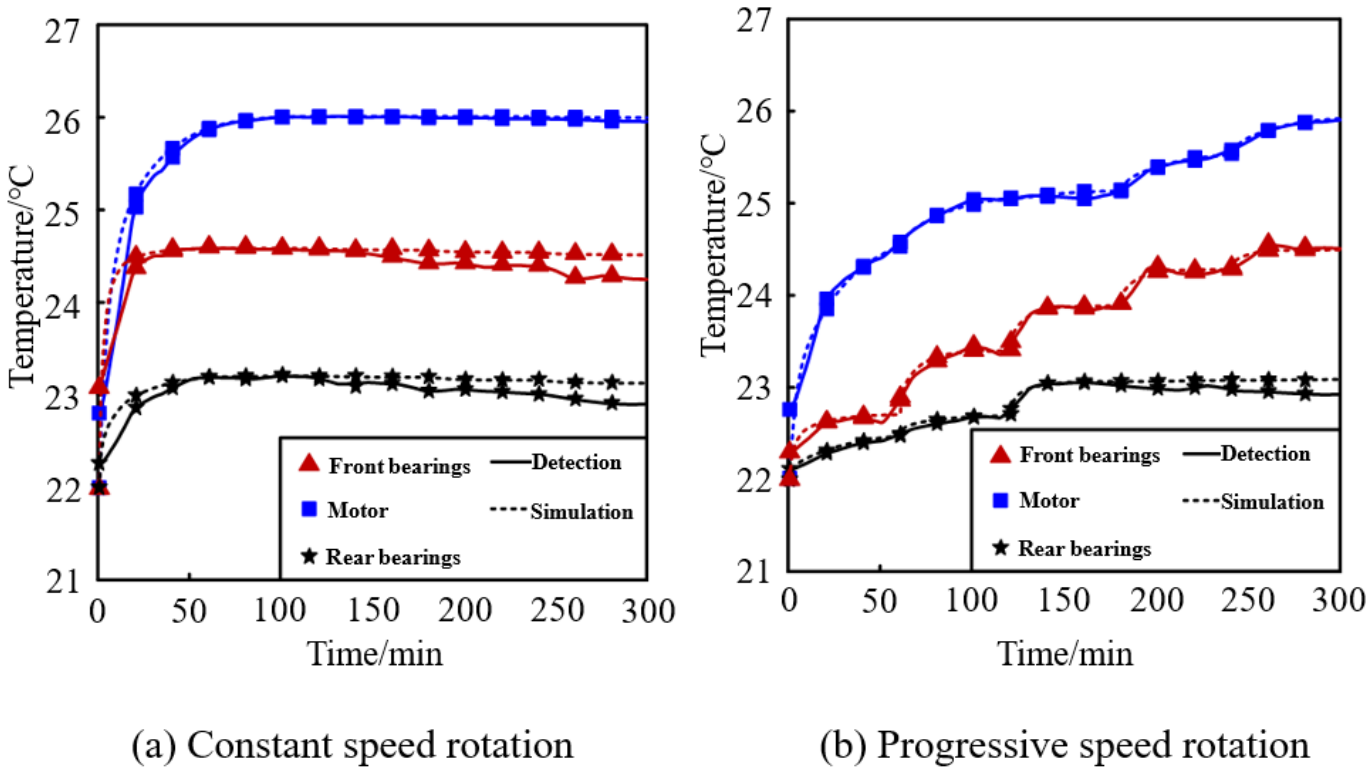

Figure 8

Simulation - detection comparisons of spindle structural temperatures

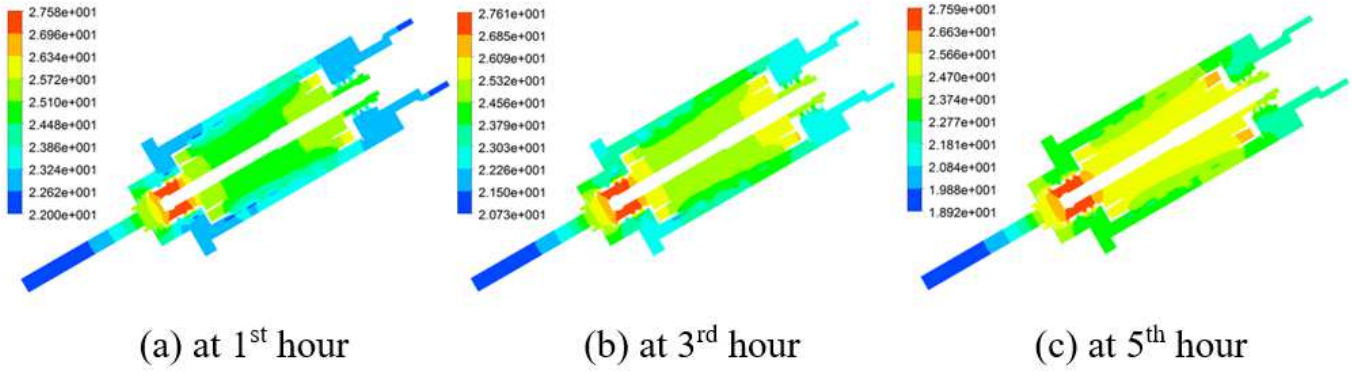

Figure 9

Simulation temperature fields of spindle structure (Constant speed rotation)

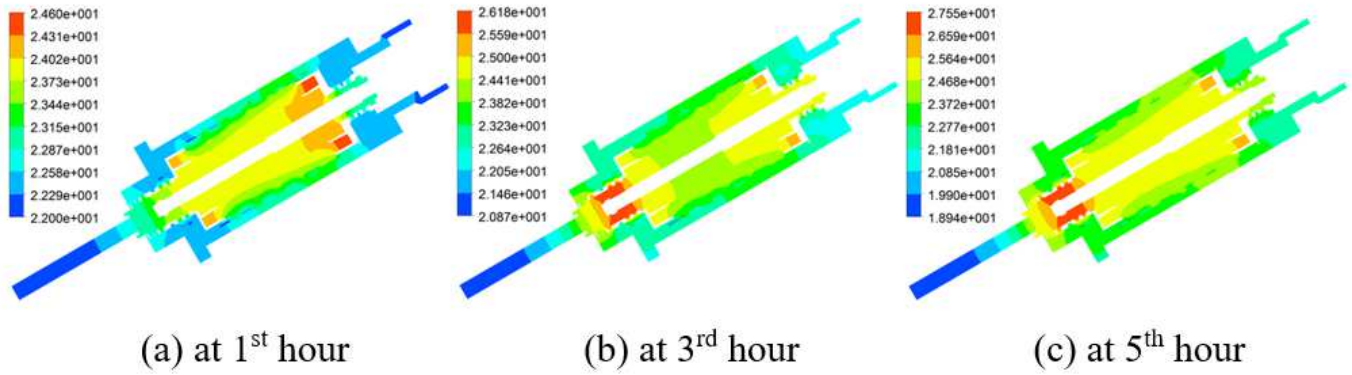

Figure 10

Simulation temperature fields of spindle structure (Progressive speed rotation)

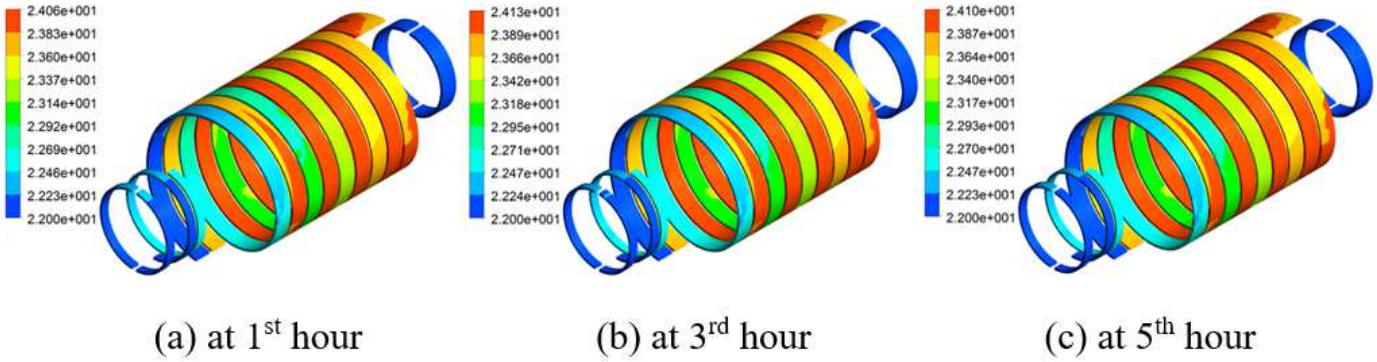

Figure 11

Simulation temperature fields of spindle coolants (Constant speed rotation)

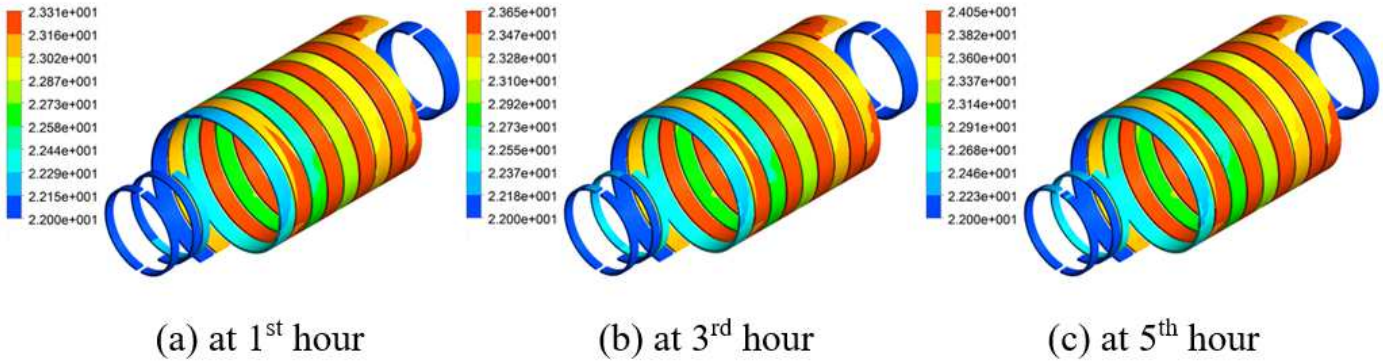

Figure 12

Simulation temperature fields of spindle coolants (Progressive speed rotation)

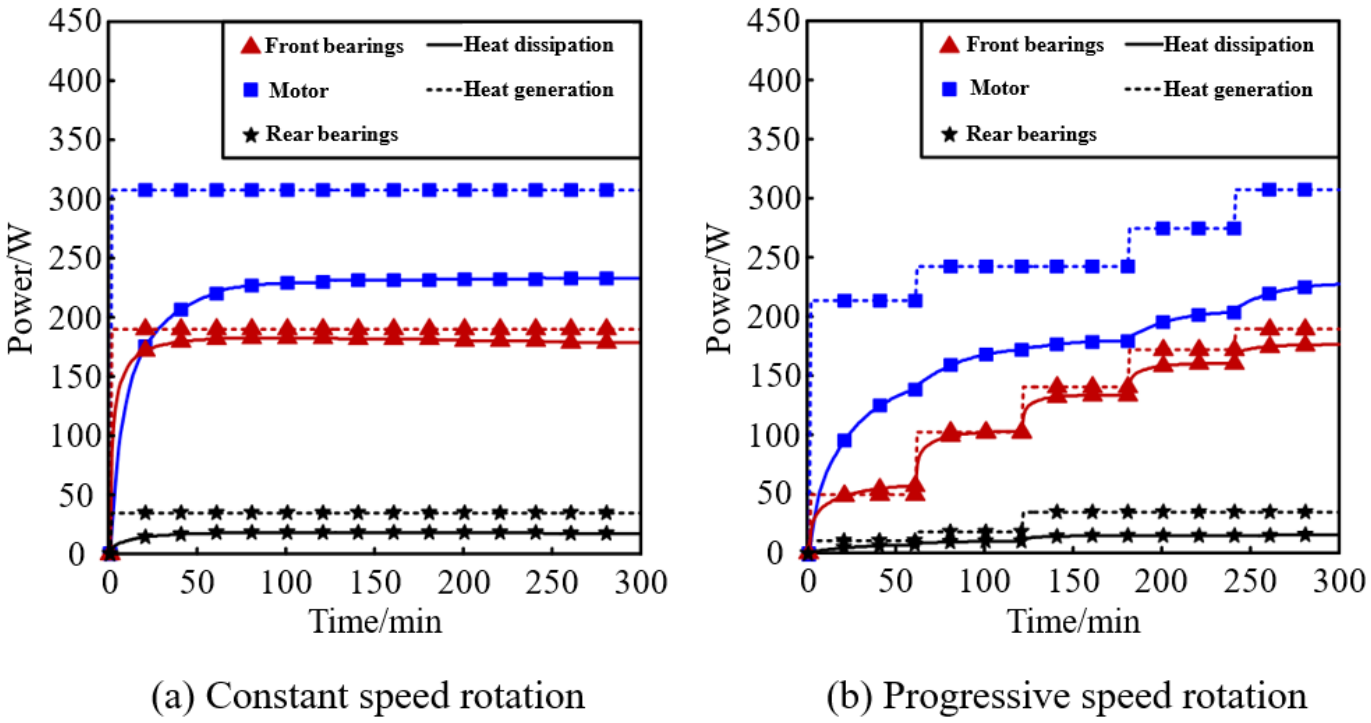

Figure 13

Power matching of spindle structural heat generations-dissipations